ENGINEERING RESEARCH INSTITUTE
THE UNIVERSITY OF MICHIGAN
ANN ARBOR

Final Report

ANTI-ICING AND ANTI-FROSTING OF AERIAL PHOTOGRAPHIC WINDOWS

M. P. Moyle
R. E. Cullen

Project 2197

U.S. AIR FORCE
WRIGHT AIR DEVELOPMENT CENTER
WRIGHT-PATTERSON AIR FORCE BASE
CONTRACT NUMBER AF 33(616)-2268

October 1955

FOREWORD

The work reported herein was conducted under The University of Michigan Engineering Research Institute Project 2197, and was monitored by the Aerial Reconnaissance Laboratory, Directorate of Laboratories, Wright Air Development Center, Wright-Patterson Air Force Base.

SUMMARY

1. Calculations were made for the deviation of a light ray passing through a boundary layer as a function of altitude and wall-to-free-stream temperature ratio. It was shown that at high flight speeds at low altitude, the deviation is significant. Cooling the wall to near the free-stream temperature reduces the deviation, but cooling the wall to below the free-stream temperature increases the deviation considerably.

2. Wind-tunnel tests were performed on a scale model of the nose of the McDonnell RF101 at Mach 1.44 to determine the pressure loading on the forward oblique window and to observe the shock configuration in the region of the forward oblique window. Schlieren pictures taken of the forward oblique window are included in this report. The experimental pressure distribution as a function of angle of attack agreed very well with the data calculated for a normal shock.

3. Investigations were made into the safety of the forward-oblique-window design for the McDonnell RF101. Calculations were made for the safety factor as a function of altitude and Mach number. At the design cruise Mach number at sea level, the safety factor was found to be approximately 2.7 when only ram-pressure loading was included. It was found that the loading due to thermal stress from the nonuniform temperature distribution resulting 10 seconds after a dive from 50,000 to 3,000 feet amounted to about half the ram loading. The safety factor was reduced from 2.7 to 1.7 by including the thermal stress. It was recommended that the design thickness of the window be increased in view of the unknown loads not included in the analysis and the uncertainties in the behavior of glass. A research program to determine the minimum safe thickness of the RF101 forward oblique window was proposed. It was pointed out that the results of the program would be applicable for future design criteria.

OBJECTIVE

The object of this investigation was (1) the analytical and experimental determination of the deviation of a light ray passing through a boundary layer and (2) the evaluation of the problem of breakage of the forward oblique window in the RF101.

TABLE OF CONTENTS

LIST OF ILLUSTRATIONS

NOMENCLATURE

τ	time
ds	arc length
$v(x,y)$	velocity distribution
y'	derivative of y with respect to x
dx	differential of x
c	velocity of light in vacuum
$n(x,y)$	refractive-index distribution
s_1	path length in medium 1
s_2	path length in medium 2
c_1	velocity of light in medium 1
x	distance
i	incidence angle in Snell's law
r	reflected angle in Snell's law
θ_i	incidence angle
θ_w	wave angle
β	angle between normal to first cell and emergent ray
δ	deviation of ray from original path
n_1	refractive-index medium 1
n_2	refractive-index medium 2
k	numerical index
δ_t	deviation of ray from original path, seconds
T_∞	free-stream temperature, °Rankine
T_w	wall temperature, °Rankine
S_x	stress in x direction, psi
P	pressure, psi
A	1/2 length of side, inches

t	thickness, inches
B	1/2 length of width, inches
M_x	bending moment, ft-pounds
β'	empirical factor used in stress formulas

INTRODUCTION

The reconnaissance versions of present-day fighter aircraft are very complex machines. In addition to the complexities that go along with the fighter aircraft, additional complexities are added by the camera installations and photographic windows. Inasmuch as the two aircraft are used for basically different missions, it might be profitable at this time to evaluate the philosophy of modifying fighter aircraft into the reconnaissance versions. A considerable saving in weight characteristics might be realized by an optimum design and camera installations might be simplified.

A considerable number of problems are associated with the camera installation and the photographic system itself. Among these are the problems of vibrationless mounts, lens design, defrosting windows, window installations, etc. A review of the photographic system and the problems associated with it was published in an earlier report.[17]

The problem of fog and frost prevention has been an important one in the past and will continue to be so, at least during portions of the flight time, in future operations. Examination of Fig. 1 shows the Mach number of flight which will maintain the windows at 85°F on the outer surface as a function of altitude. If one uses the criterion that the inner surface should be at 85°F at high altitude before entering into a dive to sea level, then the curves shown in Fig. 1 are for zero heat input. It is obvious that present aircraft cross this curve at some point during their flight. Future aircraft will undoubtedly fly for longer periods of time in the zone where no heat is required and, consequently, cooling the photographic windows will be required to reduce thermal loading and to prevent failure. For example, if one extrapolates photographic flight to Mach 2.0 at sea level, the skin temperature will rise to about 475°F. Obviously, this temperature is much too high for the type of window being used currently, but the Mach number increase is relatively small and can be foreseen in the near future. Heavy-gauge stainless-steel skins are contemplated for future aircraft to combat the so-called thermal barrier. The photographic windows either will require heat-resistant glass, such as quartz, or will require cooling. Quartz windows of the size involved and of the optical quality required would probably cost a prohibitive sum. External cooling by injection of cold air into the boundary layer is quite feasible, however. Moreover, it has the advantage, from the optical standpoint, of reducing the deviation caused by refraction through the boundary layer. The problem of refraction through the boundary layer is discussed

in the following section, and other topics investigated during the contract year are discussed in succeeding sections.

REFRACTION OF A LIGHT RAY PASSING THROUGH A LAMINAR BOUNDARY LAYER

The boundary layer in high-speed flow is a transition zone where the change from wall to free-stream temperature occurs. The transition may or may not be a linear one. Since the temperature and density change through the boundary layer, the refractive index also changes in accordance with the density. The general problem is that of a light ray passing through a two-dimensional temperature field and is a problem in the calculus of variations. The path which the light ray follows is curved in such a fashion that the time of transit through the medium is a minimum. It is known in mathematics as Fermat's principle or the principle of least time. The general equations governing the time of transit and the path are as follows:

$$\tau = \int \frac{ds}{v(x,y)} = \int \frac{\sqrt{1 + y'^2}\, dx}{v(x,y)} \qquad (1)$$

$$P = c\tau = \int \frac{c\,ds}{v(x,y)} = \int n(x,y)\,ds \qquad (2)$$

$$= \int_{x_1}^{x_2} n(x,y)\sqrt{1 + y'^2}\, dx \qquad (3)$$

The above integrals must be minimized in any application. Snell's law results as a special case of the above for a one-dimensional temperature field.

The differential equation for the two-dimensional temperature field was found to be analytically intractable. Therefore, an approximation method was devised to calculate the refraction through the boundary layer.[19] The method was long and tedious. Therefore, a further approximation was made and a considerable simplification resulted. Computations made by the two methods gave results within a fraction of a percent of each other. The analysis is as follows:

Given a one-cell system,

$$\theta_i = \beta - \delta \quad \text{or} \quad \beta = \theta_i + \delta \qquad (4)$$

using the identity,

$$\sin (x + y) = \sin x \cos y + \cos x \sin y \tag{5}$$

so,

$$n_i \sin \theta_i = n_1 \sin \theta_i \cos \delta + n_1 \cos \theta_i \sin \delta \tag{6}$$

and

$$n_i \tan \theta_i = n_1 \tan \theta_i \cos \delta + n_1 \sin \delta \, . \tag{7}$$

Now, for small values of δ,

$$\cos \delta \approx 1 \; ; \; \sin \delta \approx \delta \, .$$

Then,

$$n_i \tan \theta_i = n_1 \tan \theta_i + n_1 \delta \tag{8}$$

or

$$\frac{n_i - n_1}{n} = \delta / \tan \theta_i \, . \tag{9}$$

Extending to k cells

$$\frac{n_i - n_1}{n_1} = \delta_1/ \tan \theta_i \tag{10a}$$

$$\frac{n_1 - n_2}{n_2} = \delta_2 / \tan \theta_i \tag{10b}$$

or

$$\frac{n_{k-1} n_k}{n_k} = \frac{\delta_k}{\tan \theta_{k-1}} \tag{10c}$$

Summing over n,

$$\frac{n_i}{n_1} + \frac{n_1}{n_2} + \frac{n_2}{n_3} + + + \frac{n_{k-1}}{n_k} - k = \frac{\delta_1}{\tan \theta_i} + \frac{\delta_2}{\tan \theta_i} + + + \frac{\delta_k}{\tan \theta_k} \, . \tag{11}$$

Then, if the total deviation, δ_t, is small,

$$\tan \theta_1 = \tan \theta_2 = \tan \theta_{k-1} ,$$

and then,

$$\frac{\delta_t}{\tan \theta_i} = \sum_{k=i}^{n} \frac{n_{k-1}}{n_k} - k . \tag{12}$$

If a two-cell system is used with the Gladstone-Dale relation for variation of refractive index with temperature, $n_k = 1 + a/T_k$, we obtain,

$$\frac{\delta_t}{\tan \theta_i} = \frac{1 + A/T_\infty}{1 + A/T_w} - 1 , \tag{13}$$

or rearranging,

$$\delta/\tan \theta_i = \left(\frac{T_\infty + A}{T_w + A}\right)\left(\frac{T_w}{T_\infty}\right) - 1 , \tag{14}$$

where A is a function of altitude. The results calculated by this method agree satisfactorily with those calculated by the previous method. Figure 2 shows the results for the laminar boundary layer. The deviation is independent of Mach number and depends only on the altitude and the wall-to-free-stream temperature ratio. The curve is plotted as the deviation (seconds of arc) of the ray from its original path divided by the tangent of the angle of incidence vs the wall-to-free-stream temperature ratio (absolute), with the altitude as a parameter. The wall-to-free-stream temperatures of practical interest lie between 0.9 and 2.0. Above 2.0, the results are of academic interest only.

An examination of Fig. 2 reveals the interesting fact that when the wall temperature equals the free-stream temperature ($T_w/T_\infty = 1.0$), the function $\delta/\tan \theta_i = 0$ for all angles of incidence. Thus, a means of reducing or eliminating the error δ is available by cooling. Cooling to below $T_w/T_\infty = 1.0$, however, is to be avoided as large deviations occur in this region.

In the application of the graph, the ratio T_w/T_∞ (where T is in °Rankine) is computed at the altitude in question and the value of $\delta/\tan \theta_i$ is read from the graph (Fig. 2). The angular deviation from the original

path in seconds of arc is then obtained by multiplying by the tangent of the angle of incidence. In any camera, the deviation varies from zero on the optic axis to a maximum, depending on the cone angle. For example, consider an aircraft flying at a Mach number of 0.8 at sea level. The equilibrium surface temperature of the window would be approximately 124°F or 584°Rankine, based on the NACA standard atmosphere. The free-stream temperature would be 59°F or 519°Rankine. The ratio T_w/T_∞ would be 1.13 and from Fig. 2 $\delta/\tan \theta_i$ would be 5.0. For a lens with a 45° half-cone angle, the maximum deviation would be 5.0 seconds at the edge. If a guided missile were used for carrying the photographic equipment, the Mach number of flight would undoubtedly be supersonic. For a Mach 3.0 missile and the same lens, the deviation δ experienced would be 38 seconds, neglecting the effect of shock waves.

In the case of shock waves, the refraction effect is probably even more severe due to the density shift which increases with the shock strength. Moreover, such a shock configuration would probably be of a conical nature dependent upon the geometry of the aircraft. In such a shock configuration, the placement of the camera becomes important. The more nearly perpendicular the optic axis is to the shock, the less the deviation. A preliminary attempt was made to determine the deviation through the shock wave off the Pitot mast of the RF101 and in front of the forward oblique window at a 1.3 flight Mach number. The Pitot mast half angle was assumed to be 5°. From the tables in Reference 5, the wave angle, θ_w, was found to be 60°, if the body was considered to be a wedge. This corresponds roughly to the actual case as seen in Fig. 6, which is a schlieren picture of the flow past a scale model of the RF101 at 1° angle of attack in a Mach 1.44 stream. Figure 5 shows the model set up in the tunnel. Figures 6, 7, and 8 are schlieren pictures of the model at 0, 1, and 2° angle of attack. Figure 9 is a schlieren picture of the flow past the model, looking down from above and at 11° angle of attack. The shock configuration is fairly planar ahead of the forward oblique window, but rounds out into a conical form rapidly. On the assumption that the density gradient through the shock in front of the forward oblique window is one dimensional, the deviation at Mach 1.3 is approximately as shown in Fig. 4, a more rigorous analysis is required to determine the effect of the shock wave on the photographic quality obtainable at supersonic speeds. Schlieren pictures of the RF101 nose model should be obtained at Mach numbers between 0.5 and 1.5 to see just what the shock configuration is in the neighborhood of the nose area.

The experimental investigation of light refraction through the boundary layer has progressed slowly due to the priority of other work. The apparatus as described in a previous progress report has been modified slightly (Fig. 3). Since considerable drift was experienced with the 931A photomultiplier tube, a cadmium sulfide cell was substituted and very good reproduction of results has been obtained with this type of photosensitive element. Other sources of difficulty have been the bending of the test window during heating and the second boundary layer, which develops on the opposite side of the test window. This second boundary layer tends to cancel out the effects of the first. A vacuum cell has been designed to

eliminate the second boundary layer. Initial calibrations of the apparatus indicate that measured deflections through curved plexiglas specimens are of the same order of magnitude as calculated values. A further refinement is required, however, to detect the small angles associated with the boundary layer.

THE AIRCRAFT GLASS PROBLEM

As mentioned in a previous section, the aircraft window problem is becoming acute as flight speeds increase and window-size requirements go up. The problem in the photographic aircraft at high flight speeds is twofold; (1) the windows are subjected to high skin temperatures and (2) forward windows are subjected to large ram pressures.

The ram-pressure problem has already been experienced, with up to one-inch windows being required in some installations. At present, the skin temperatures developed are not so excessive as to prohibit the use of ordinary glass, but a small increase in operating Mach number could bring about such a situation. The situation can be alleviated, however, by boundary-layer injection of cold air to maintain the window surface cool.

In order to maintain windows of moderate thickness, window area and location will have to be restricted. This points again to the need for a "pure" design for the photographic aircraft. The problem of specifying a minimum safe thickness for the forward oblique window in the RF101 has already been experienced by McDonnell. In the past, a large "ignorance" factor has been included in any design involving glass, due to the uncertainty of the mechanical properties of glass. As window-thickness requirements go up, this factor appears to add excess weight to the aircraft, which already is heavier than desirable. Thus, the tendency to cut back upon the "ignorance" factor is apparent. The "ignorance" factor is justified when one examines just what it means. For example, in the RF101 design, the safety factor for the forward oblique window was found to be approximately 2.7 (the method of calculation is shown in Appendix I) due to steady-state ram-pressure loading alone at the design cruise Mach number. Many factors contributing to stress concentrations were neglected in arriving at the safety factor of 2.7. A few of these are:

1. Local mechanical loading at the frame

2. Thermal stress of the edge induced by a cold or hot frame

3. Local stress from hot spots in the Liberty 81E conductive coating, due to nonuniformities in the conductive sheet or to scratches in the coating

4. Impact loading by precipitation

5. Scratches and abrasion

6. Inertial loading.

During a dive to sea level, the window will go through a considerable temperature history, as can be seen in Fig. 17 of Reference 18. Figure 12 of this report shows the temperature distribution through the forward oblique window ten seconds after diving to 3000 feet from 50,000 feet. A nonlinear temperature distribution, such as that shown in Fig. 12, gives rise to a stress loading in addition to the ram-pressure loading. A thermal stress is set up in the window; the stress distribution is shown in Fig. 13. Reference to Fig. 13 shows that the outside surface of the window is in compression, while the inside surface is in tension. The thermal loading then is additive to the ram loading. The net effect of the thermal loading is to reduce the safety factor from 2.7 to 1.7 at the cruise Mach number of 0.8. It was not possible to construct safety-factor curves as a function of Mach number, including the thermal loading, since the temperature distributions through the window at Mach numbers other than 0.8 were not available.

In view of the above, it would appear that the design thickness of 1/2 in. is insufficient, especially when one considers that scratches can reduce the safety factor by a factor of 2. Furthermore, the cruise Mach number is considerably less than the maximum possible. Reference to Fig. 10 for the 1/2-in. window indicates that the window would fail due to ram pressure alone at about Mach 1.2 at sea level. The thermal loading would probably reduce this to Mach 1.1. A comparison of the RF101 installation with the RF84F was made to determine the magnitude of the "ignorance" factor included in the RF84F design. The forward oblique window of the RF84F, aircraft was much smaller than that of the RF101 (9.56 by 10 in., as compared with a trapezoidal shape a = 9 in., b = 17 in., h = 17 in.). The thickness of the two installations, however, is the same, i.e., 1/2 in. In the case of the RF84F, the safety factor is approximately 9 at the cruise Mach number of the RF101. Inasmuch as the RF84F cruise Mach number is probably lower than that of the RF101, the difference is probably even greater. Thus, it can be seen that the glass industry's rule-of-thumb safety factor of 10 has probably been applied in the case of the RF84F and is sufficient to cover the thermal loading involved.

In order to check the accuracy of the estimation of the ram-pressure loading on the RF101 forward oblique window, a scale model of the nose was fabricated and tests were performed in the University of Michigan Supersonic Wind Tunnel* (Reference 4). The pressure distribution as a function

*The University of Michigan Supersonic Wind Tunnel is under the direction of H. P. Liepman of the Aeronautical Engineering Department. The assistance extended by Dr. Liepman and J. Amik in obtaining the schlieren pictures and pressure data is gratefully acknowledged.

of angle of attack was determined at Mach 1.44. The results are shown in Fig. 14. The calculated values, using normal shock relations, yield values to a fraction of a percent of those measured.

A conference was held on August 15 and 16, 1955, at the McDonnell Aircraft Co. to discuss the problem of the RF101 forward oblique window with McDonnell Aircraft and Wright Field personnel. The curves shown in Figs. 10 and 11 were presented and the uncertainties involved in the properties of glass were pointed out. Those attending the meeting appreciated the fact that a design safety factor of 10 might be only an actual value of 1.5, as far as the aircraft were concerned. University of Michigan personnel recommended that a 1-in.-thick window be substituted for the 1/2-in.-thick window planned. Reference to Fig. 11 indicates that the aircraft is out of the danger zone with a 1-in.-thick window. McDonnell personnel indicated that a 3/4-in.-thick window could be installed without a major design change, but 1-in.-thick windows would involve design changes. A compromise was arrived at temporarily to install 3/4-in.-thick windows until sufficient information could be gathered to set satisfactorily a safe working safety factor. The safety factor for the 3/4-in.-thick window would be roughly 5 for the design cruise Mach number, which is still somewhat marginal, considering the possibility of higher flight speeds. The thermal loading is not known precisely since the temperature distribution for a 3/4-in.-thick window was not available.

A second conference concerning the window problem was held at WADC on August 23, 1955, to discuss the problem with Wright Field and Libbey-Owens-Ford personnel. The general problem of the RF101 forward oblique window was reviewed for those not present at the meeting with McDonnell, and new problems connected with the Liberty 81E conductive coating were brought to light. Libbey-Owens-Ford personnel indicated that hot spots were developed near the terminal points of the bus bars on nonrectangular windows. The thermodifferential tests reported by Miller[14] were also discussed. A program of research to answer the above problems was outlined and generally agreed on. The program would consist of three phases: Phase I would consist of an investigation of the geometry effect by testing geometrically similar specimens of 1/8-, 1/4-, and 1/2-in.-thickness windows, which retain a constant area-to-thickness ratio and would be the exact shape of the RF101 forward oblique window; Phase 2 would consist of the investigation of the effect of coating discontinuities on the breaking strength. The magnitude of hot spots in the vicinity of scratches also would be investigated. In Phase 3, the effect of bus-bar geometry on heat generation would be examined. Finally, a number of 3/4-in.-thick coated windows (or the thickness deemed necessary if the preliminary tests indicate a value different from 3/4-in.) would be tested completely. The number of 3/4-in.-thick windows would depend on the information gained in Phases I, II, and III and upon the funds available for the purchase of test specimens. A test setup has been fabricated which can simulate ram-pressure and thermal loading. It is believed that controlled ram and thermal loadings can be accomplished and, thus, actual flight simulation may be possible. No ex-

perimental work has been performed on this phase, awaiting official sanction of the Air Force.

The analytical investigation of the effect of scratches on the current distribution and temperature attained in the neighborhood of a scratch was initiated. An analogy can be made between the flow of fluid and the flow of electric current in a conductive sheet since, for steady irrotational flow, both potentials obey Laplace's equation. The flow about a line perpendicular to the direction of flow (a scratch parallel to the bus bars) can be obtained by a transformation of the flow about a line parallel to the flow into the flow about a circle and, thence, the transformation of the flow about the circle into the flow about a line perpendicular to the flow. The flow about a line at any degree to the flow can be obtained in a similar manner. This technique has been established.

It should be pointed out at this time that the glass problem is not restricted to the photo-reconnaissance aircraft and its photographic windows. All aircraft windshields are subject to the same problem. A typical example of glass failure has been experienced in the F86 armor-plate windshields. Armor-plate windshields in the F86 are made up of alternate laminations of glass and plastic to create a 1-1/4-in.-thick shatter-proof window. A number of these cracked in aircraft used during the Korean campaigns, when the hot-air anti-icing systems were turned on. Fortunately, the laminate type of construction prevented complete disintegration of the window. The reason for failure of the F86 windshield appears to have been due to thermal loading in conjunction with cabin-pressure loading. An investigation of the problem[7] indicated that window failure occurred when an outer-surface temperature of 220°F was reached. A redesign of the air-supply nozzles is said to have solved the particular problem. However, a skin temperature of 220°F due to friction alone will be attained in steady flight at about Mach 1.5, and the problem could arise again.

ANTI-FOGGING OF HIGH-ALTITUDE HEADGEAR

The investigation of the problem of anti-fogging high-altitude headgear was undertaken for the Aeromedical Laboratory, WADC, under the authorization of the project officer for contract AF 33(600)-2268. A report was issued[5] which discusses this problem and its possible solutions.

RESULTS AND CONCLUSIONS

The deviation of a light ray from its original path has been calculated for the case of laminar boundary layers and for a particular shock-wave configuration. The results of the calculations for the boundary-

layer analysis are plotted as the ratio $\delta/\tan \theta_i$ vs the wall-to-free-stream temperature ratio, with altitude as parameter. Inspection of Fig. 2 shows that at sea level the deviation is significant at the very low wall-to-free-stream temperatures and also at the higher wall-to-free-stream temperature ratios. The deviation vanishes at a T_w/T_∞ of 1.0. The wall-to-free-stream temperature ratios of practical interest lie between 0.9 and 2.0. Values outside this range are of academic interest only. As the altitude is increased, the value of the deviation diminishes. It is apparent that wide-angle cameras installed in high-speed aircraft operating at low altitude will suffer the most serious deviations.

With respect to the aircraft glass problem, Figs. 10 and 11 show the safety factor vs Mach number for ram-pressure loading only on the forward oblique window of the RF101. The thermal loading was found to be approximately half the ram-pressure loading 10 seconds after a dive to 3000 feet from a 50,000 foot altitude. It was concluded in this phase of the study that the original specification of 1/2-in.-thick windows was not sufficient, considering the other unknown stresses involved and the unpredictability of glass as an engineering material.

A program was recommended to determine the minimum safe thickness for the forward oblique window of the RF101. The program as planned is expected to answer the problem with respect to the RF101 and to provide a basis for future design criteria.

REFERENCES

1. Baskins, L. L. and Hamilton, L. E., "Preliminary Wind Tunnel Investigation of the Optical Transmission Characteristics of a Supersonic Turbulent Boundary Layer," Report GM-127(AM-170), Revision No. 1, Northrup Aircraft, Inc., Hawthorne, Calif., April 1952.

2. Baskins, L. L. and Hamilton, L. E., "The Effect of Boundary Layer Thickness upon the Optical Transmission Characteristics of a Supersonic Turbulent Boundary Layer," Report NAI-54-756, Northrup Aircraft, Inc., Hawthorne, Calif., November 1954.

3. Bliss, G. A., Calculus of Variations. Chicago: Open Court Publishing Co., 1925.

4. Culbertson, P. E., "Calibration Report on the University of Michigan Supersonic Wind Tunnel," Engineering Research Institute, Project D 92, University of Michigan, June 1952.

5. Cullen, R. E., Moyle, M. P., and Glover, H. G., "Antifogging Requirements for High Altitude Headgear," WADC Technical Note 55-352, July, 1955.

6. Dailey, C. L. and Wood, F. C., Computation Curves for Compressible Fluid Problems. New York: John Wiley and Sons, Inc., 1949.

7. Dunham, J. A., "Development Test of Windshield Armor Glass Anti-Icing Nozzle to Prevent Glass Cracking Due to Thermal Shock," Report NA 52-918, North American Aircraft Co., Los Angeles, September 1952.

8. Durand, W. F., Aerodynamic Theory, vol. 1. Berlin: Julius Springer, 1934.

9. Dyke, M., "The Mechanical Properties of Glass," Library Bibliography No. 111, Royal Aircraft Establishment, Farnsborough, 1954.

10. Hampton, W. M., "The Thermal Endurance of Glass," J. Soc. of Glass Technology, vol. 20, 461-74 (1936).

11. Holland, A. J. and Turner, W. E. S., "The Effect of Width on the Breaking Strength of Sheet Glass," J. Soc. of Glass Technology, vol. 20, 72-83 (1936).

12. Holland, A. J. and Turner, W. E. S., "The Breaking Strength of Glass. The Effect of Flaws and Scratches," J. Soc. of Glass Technology, vol. 20, 279-300 (1936).

13. Liepman, H. W., "Deflection and Diffusion of a Light Ray Passing Through a Boundary Layer," Douglas Aircraft Co., Report SM 14397, Santa Monica, Calif., May 1952.

14. Miller, D. J., "Tests of Thermo-Differential Limits of Glass Coated with Libbey-Owens-Ford, 81E Conductive Coating," Internal Memorandum, Aerial Reconnaissance Laboratory, WADC, December 1954.

15. Morey, G. W., The Properties of Glass. New York: Reinhold Publishing Corp., 1938.

16. Morley, A., Strength of Materials. London: Langmans, Green, and Co., 1954.

17. Moyle, M. P., Little, F. K., and Cullen, R. E., "A Review of Aircraft Photographic Systems," University of Michigan, Engineering Research Institute, Project 2197, July 1954.

18. Moyle, M. P., Little, F. K., and Cullen, R. E., "Thermodynamic Evaluation of the Installation of Electrically Conductive Coated Photographic Windows on the McDonnell RF101," University of Michigan, Engineering Research Institute, Project 2197, September 1954.

19. Moyle, M. P., Little, F. K., and Cullen, R. E., "Anti-Icing and Anti-Frosting of Aerial Photographic Windows," University of Michigan, Engineering Research Institute, Project 2197, October 1954.

20. Murgatroyd, J. B., "Thermal Endurance Tests for Glassware," J. Soc. of Glass Technology, vol. 20, 511-16 (1936).

21. Phillips, C. J., Glass, The Miracle Maker. New York: Pitman Publishing Corp., 1948.

22. Prandtl, L., and Tietjins, O. G., Fundamentals of Hydro and Aeromechanics. New York: McGraw-Hill Book Co., Inc., 1934.

23. Kesnick, I. L. and Mould, R. E., "The Use of Wire Resistance Strain Gauges and a Polarising Microscope to Determine Permanent Stresses in Tempered Glass," J. Soc. of Glass Technology, vol. 35, 487-89 (1951).

24. Schönborn, H., "General Methods of Determining the Thermal Endurance of Glass," J. Soc. of Glass Technology, vol. 20, 475-97 (1936).

25. Smekal, A., "The Influence of Specimen Width on the Breaking Strength of Sheet Glass," J. Soc. of Glass Technology, vol. 20, 449-53 (1936).

26. Timoshenko, S. and Goodier, J. N., Theory of Elasticity. New York: McGraw-Hill Book Co., Inc., 1934.

27. Timoshenko, S., Theory of Plates and Shells. New York: McGraw-Hill Book Co., Inc., 1940.

APPENDIX I

FORMULAS FOR STRESS CALCULATIONS

A. Assumptions:

(1) Uniformly distributed load

(2) Simply supported rectangular plate

B. Factors Ignored:

(1) Inertia loading

(2) Local mechanical loading at the frame

(3) Thermal stress at the edge induced by a cold frame

(4) Local stress from hot spots in coating or coating failure

(5) Impact loading by precipitation

(6) Scratches and abrasion

C. Working Formulas for Ram-Pressure Loading:

(1) Square plate (Morley): $S_x = P\ A^2/T^2$

Where P = pressure

A = 1/2 length of side

T = thickness

(2) Rectangular plate (Morley): $S_x = 2\ A^2/A^2 + B^2\ P\ B^2/T^2$

(3) Square plate (Timoshenko): $M_x = \beta' QA^2$

$S_x = 6\ \beta' QA^2/H^2$

Where Q = pressure

A = length of side

H = thickness

β' = factor

(4) Rectangular plate (Timoshenko): $M_X = \beta' Q A^2$

$S_X = 6\,\beta' Q A^2/H^2$

D. Comparison Between Square and Rectangle:

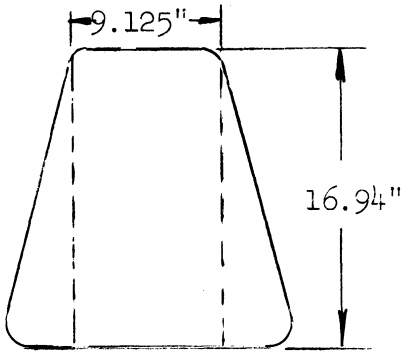

For square: $\beta = .0479$ B/A = 1.0

$S_X = 6(.0479)Q(16.94)^2/H^2$

For rectangle: $\beta = .0948$ for B/A = 1.8 = .0967 for B/A = 1.85

= .0985 for B/A = 1.9

$S_X = 6(.0967)Q(9.125)^2/H^2$

$S_X \square / S_X \square = (.0479)(16.94)^2/(.0967)(9.125)^2 = 1.71$

Use $S_X \square / S_X \square = 1.5$

Then $S_X = \dfrac{(1.5)(.0967)(6)(7.7)(9.125)^2}{\left(\frac{1}{2}\right)^2} = 2230$

E. Working Formulas for Loading due to Thermal Stress:

Assumptions:

(1) Temperature distribution function of y (the thickness) only:

(2) Simply supported rectangular plate

$$\sigma_x = \sigma_y = -\frac{\alpha E}{1 - v}\left[T + \frac{1}{2c}\int_{-c}^{c} T\,dy + \frac{3y}{2c^3}\int_{-c}^{c} Ty\,dy\right]$$

$$\sigma_z = 0.$$

Where α = coefficient of linear expansion, 99×10^{-7}

E = Young's modulus, 10×10^6 psi

v = Poisson's ratio, 0.22

c = 1/2 of thickness = 1/4 inch

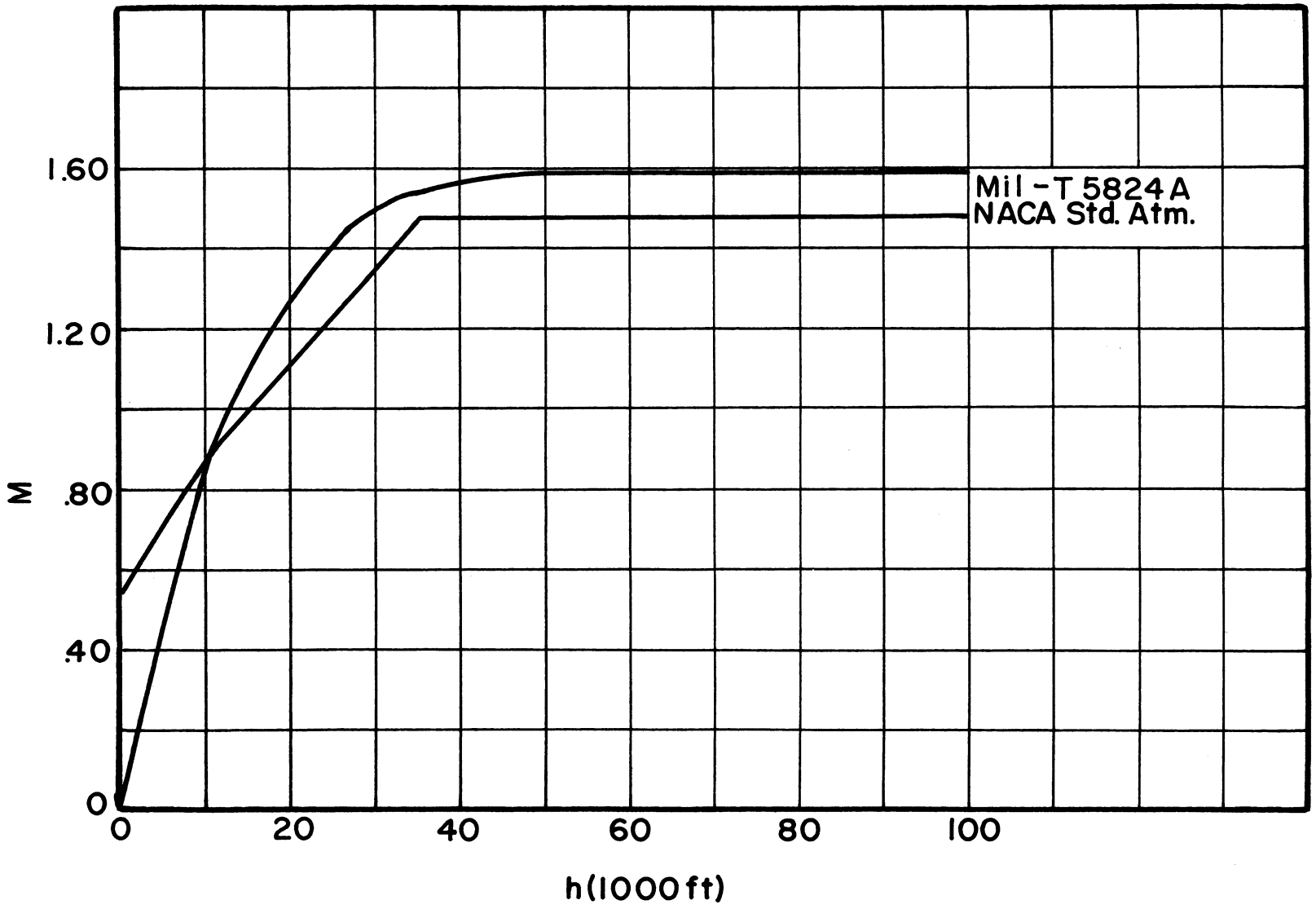

Fig. 1. Equilibrium surface temperature as a function of Mach number and altitude.

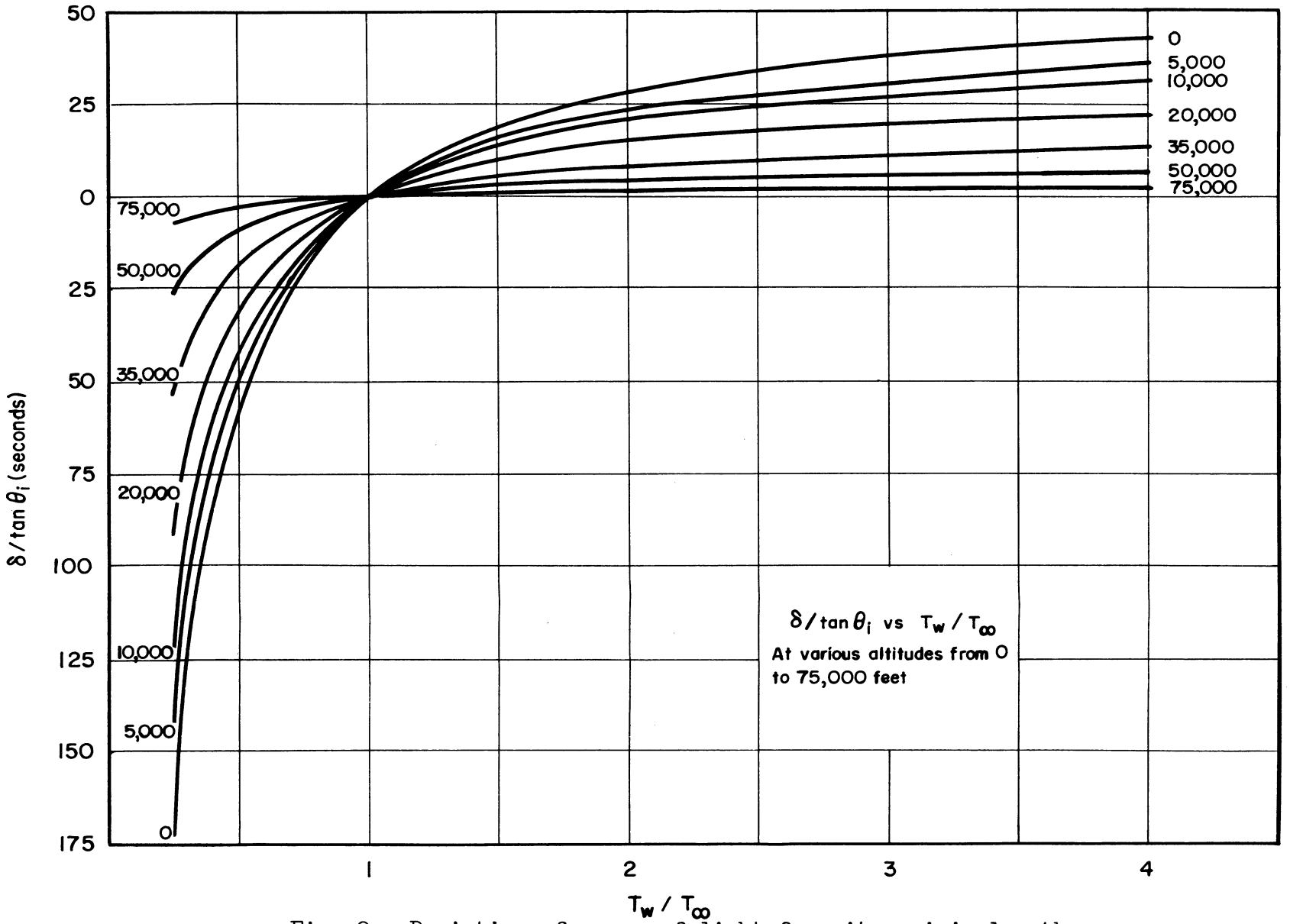

Fig. 2. Deviation of a ray of light from its original path on passing through a boundary layer.

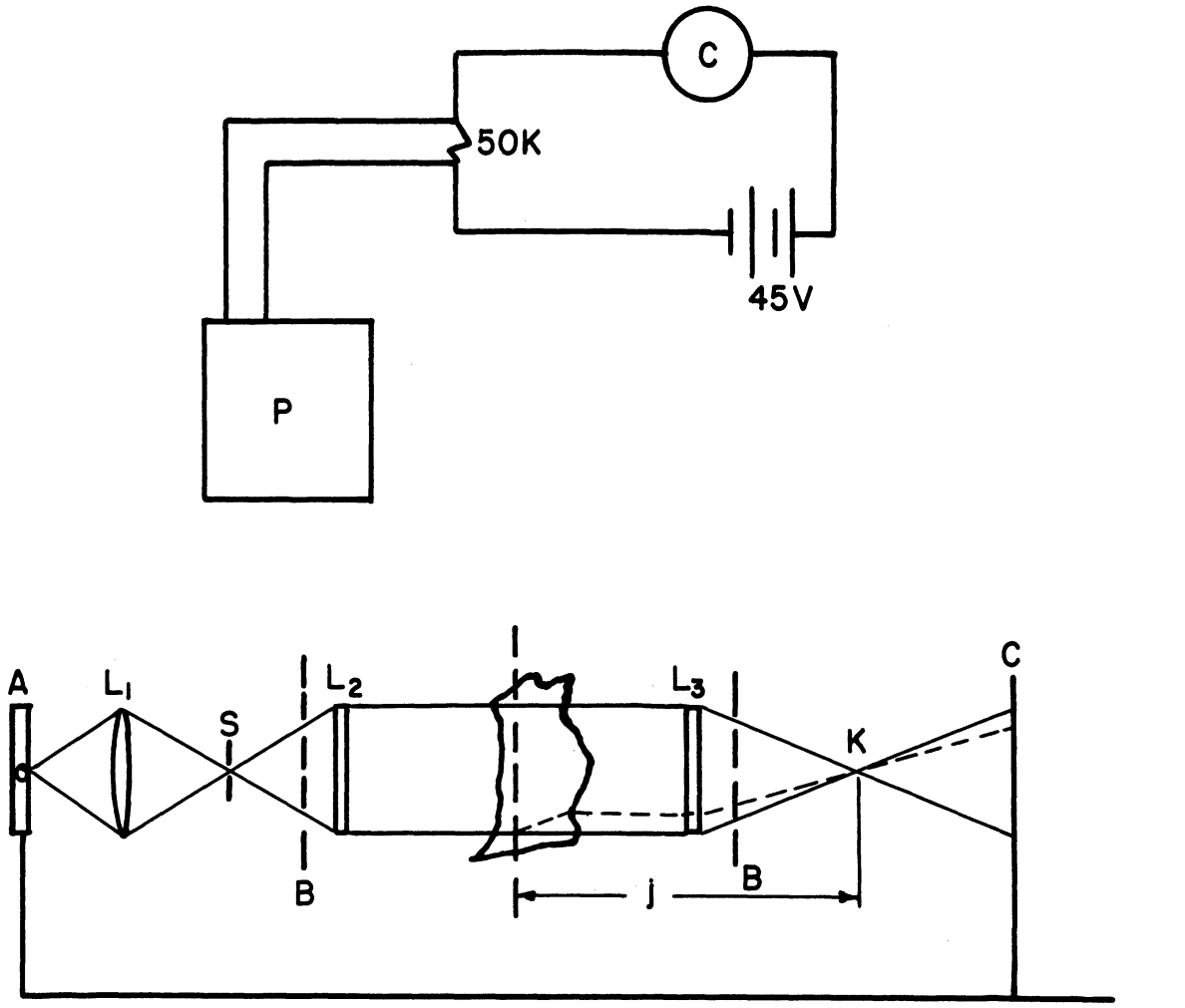

Legend

A-MERCURY LAMP
L_1-COLLECTING LENS
S-SLIT
L_2-COLLIMATING LENS
B-B-TEST SECTION
L_3-FOCUSING LENS
K-KNIFE EDGE
C-CADMIUM SULFIDE PHOTO CELL
j-DISTANCE FROM KNIFE EDGE TO DISTURBANCE
P-POTENTIOMETER

Fig. 3. Two-lens schlieren system and photocell circuit.

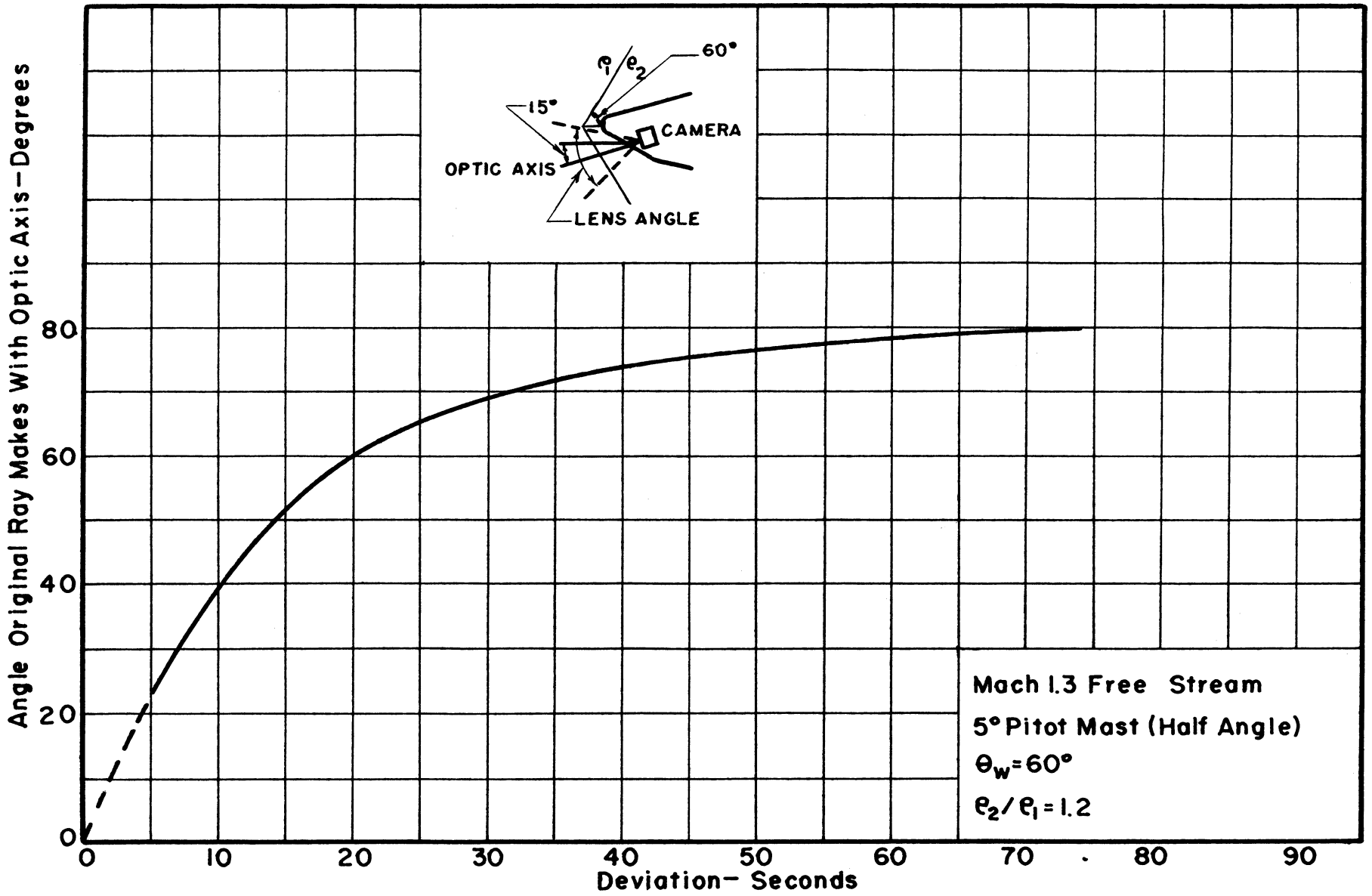

Fig. 4. Angular deviation through shock of RF101 Pitot mast at Mach 1.33.

Fig. 5. RF101 nose model setup in the University of Michigan Supersonic Wind Tunnel.

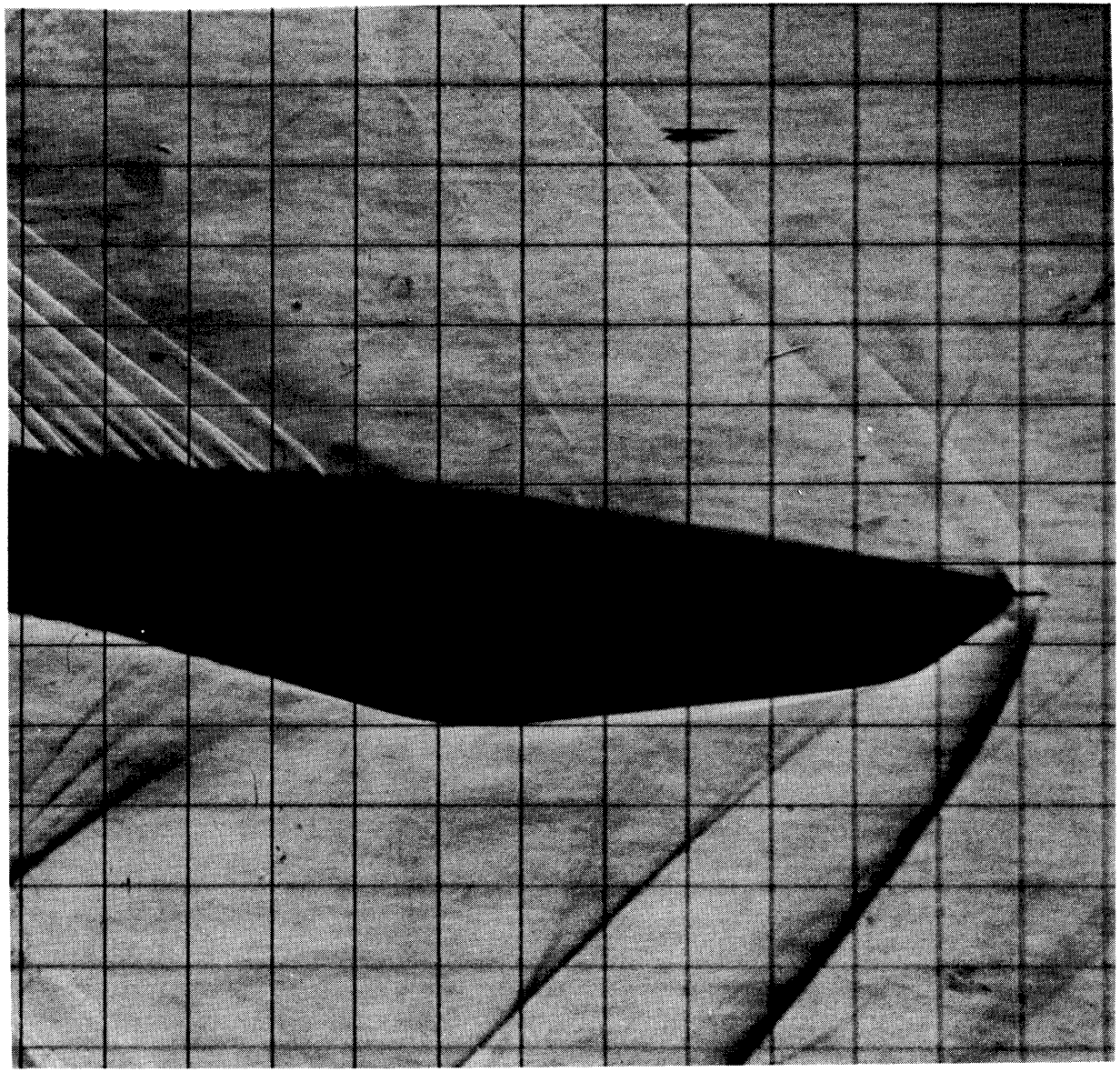

Fig. 6. Schlieren photograph of RF101 nose model in Mach 1.44 flow at 1° angle of attack.

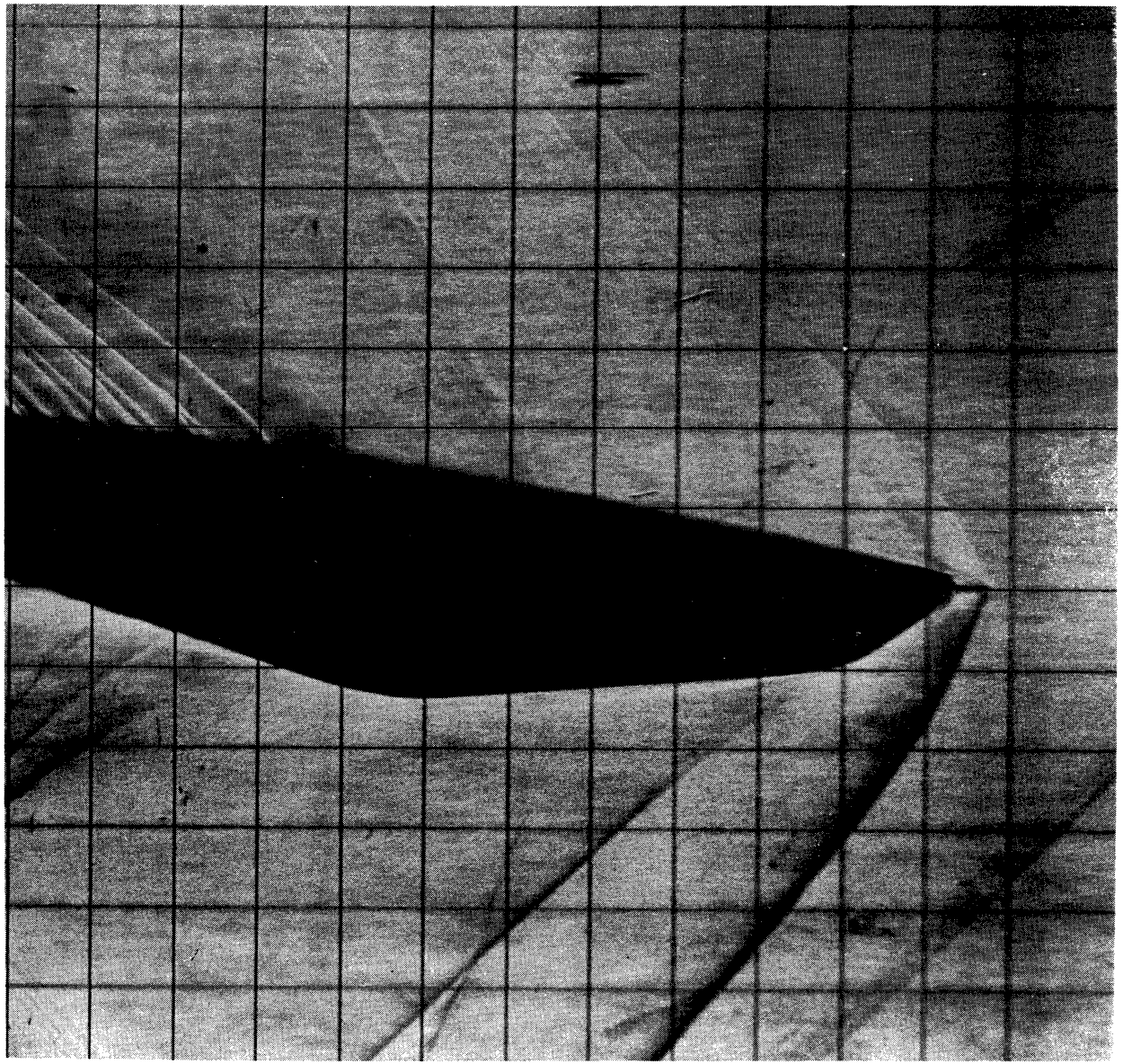

Fig. 7. Schlieren photograph of RF101 nose model in Mach 1.44 flow at 1° angle of attack.

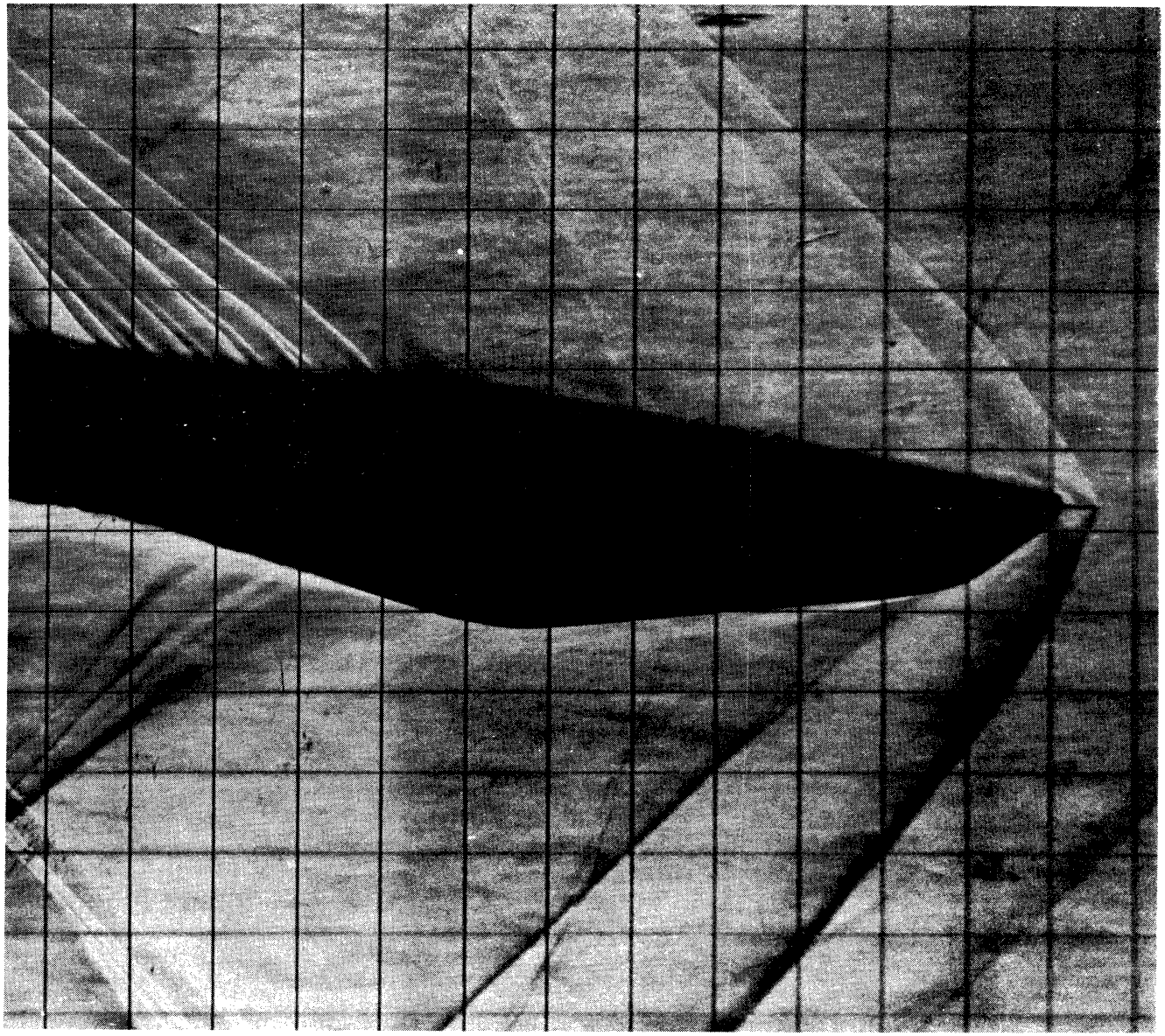

Fig. 8. Schlieren photograph of RF101 nose model in Mach 1.44 flow at 2° angle of attack.

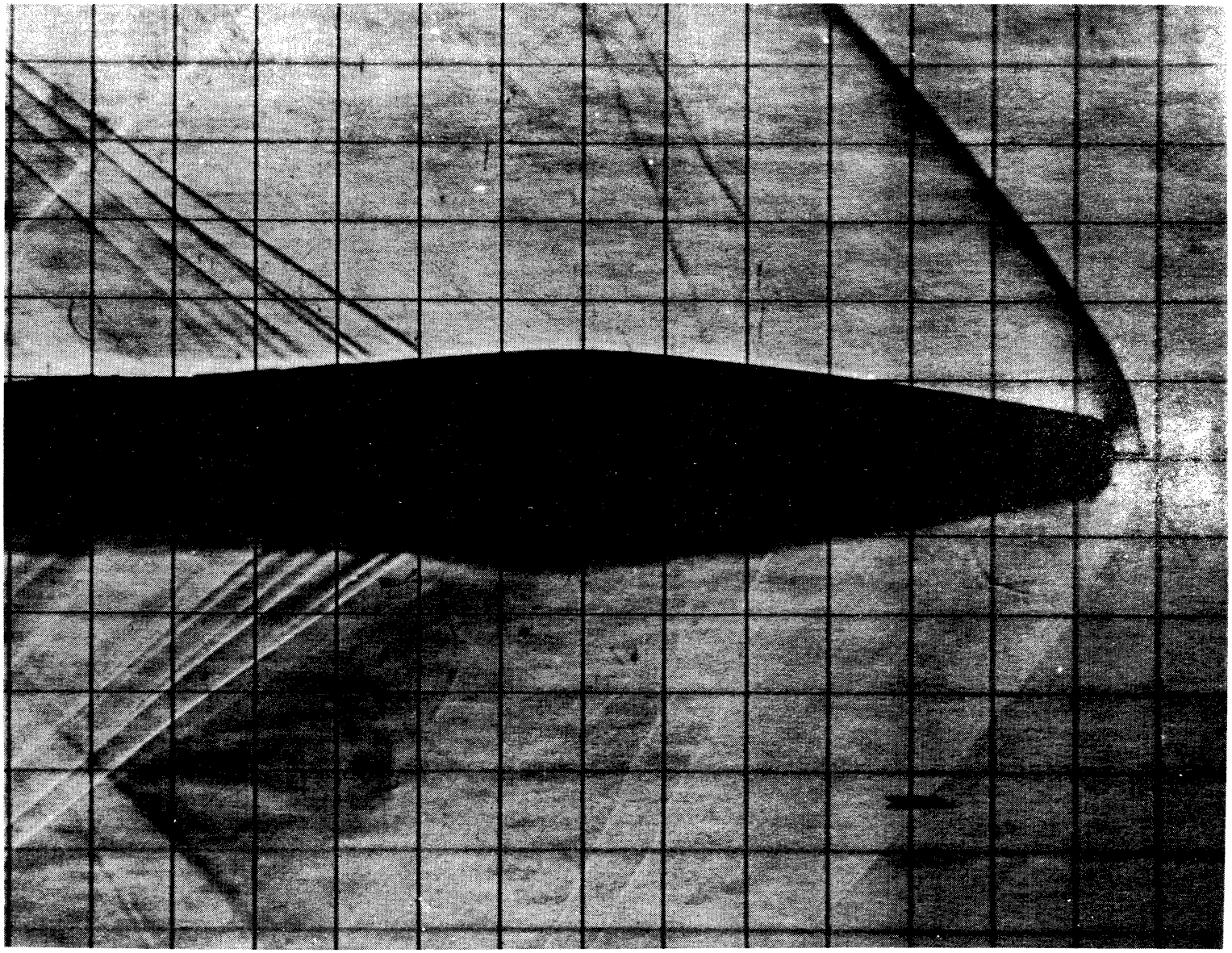

Fig. 9. Schlieren photograph of the RF101 nose model in Mach 1.44 flow at 11° angle of attack (top view).

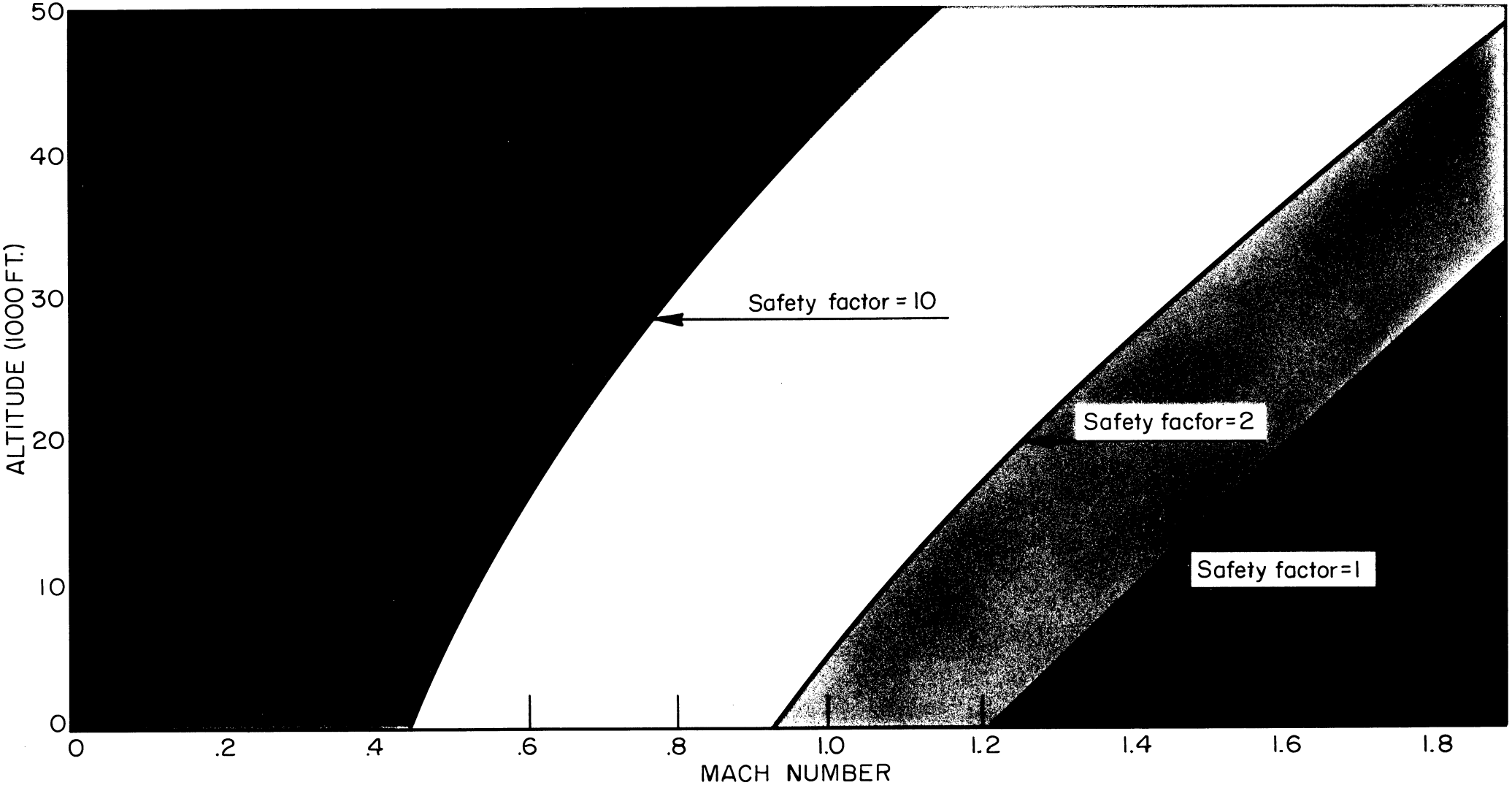

Fig. 10. Safety-factor curves for ram loading only, 1/2-inch window.

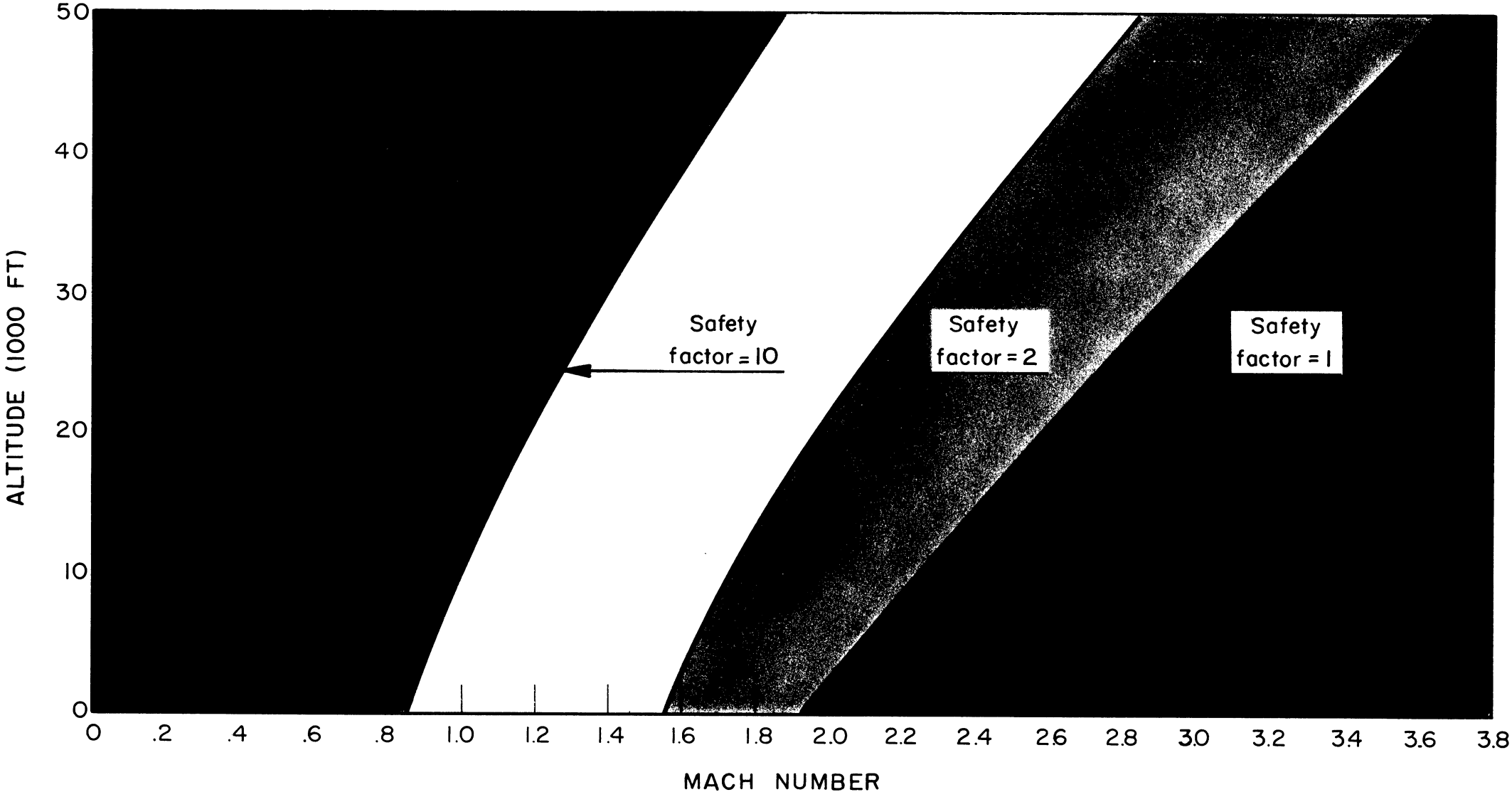

Fig. 11. Safety-factor curves for ram loading only, 1-inch window.

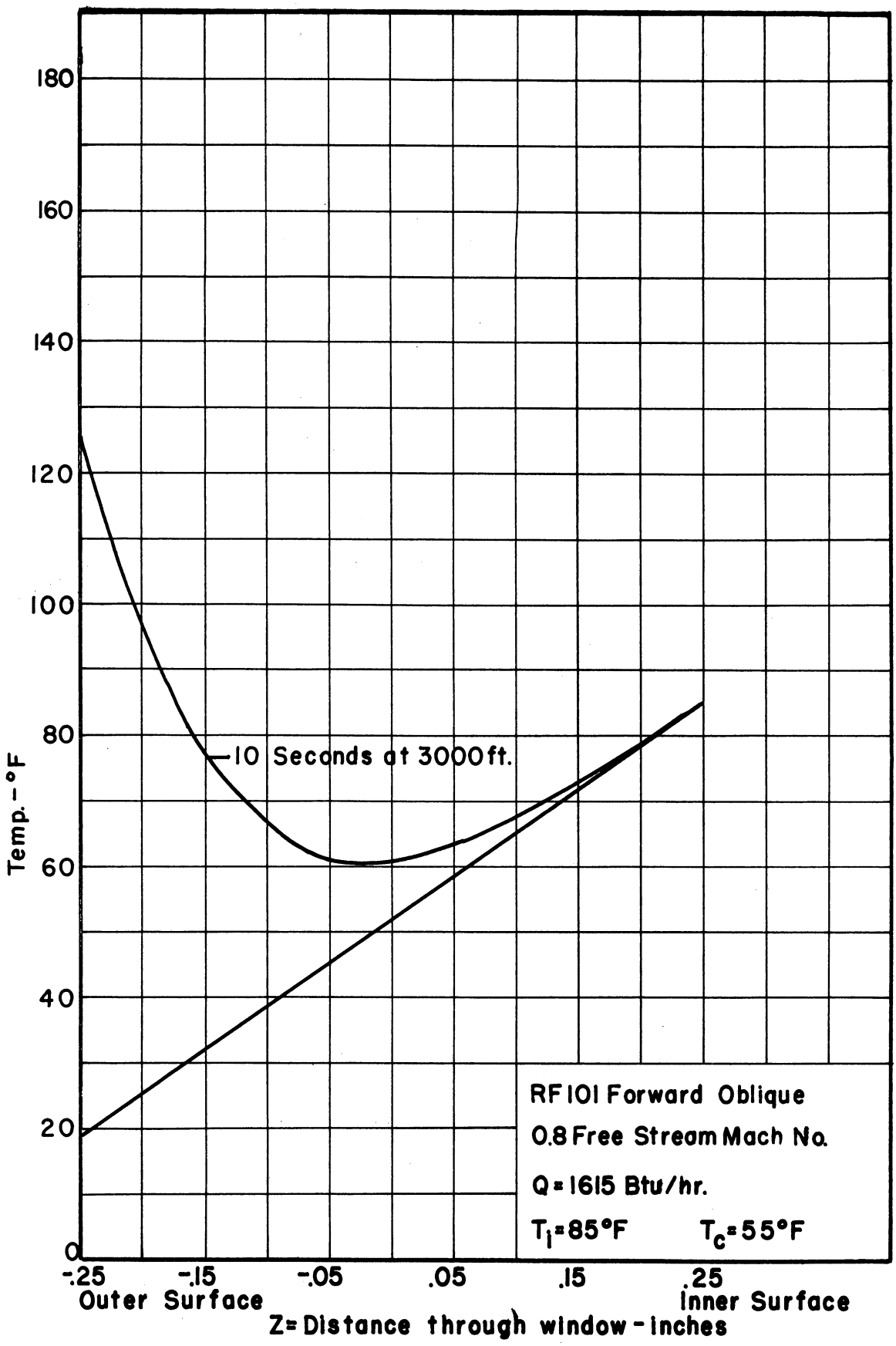

Fig. 12. Temperature distribution through the forward oblique window of the RF101, 1/2 inch thick, 10 seconds after dive from 50,000 ft to 3000 ft.

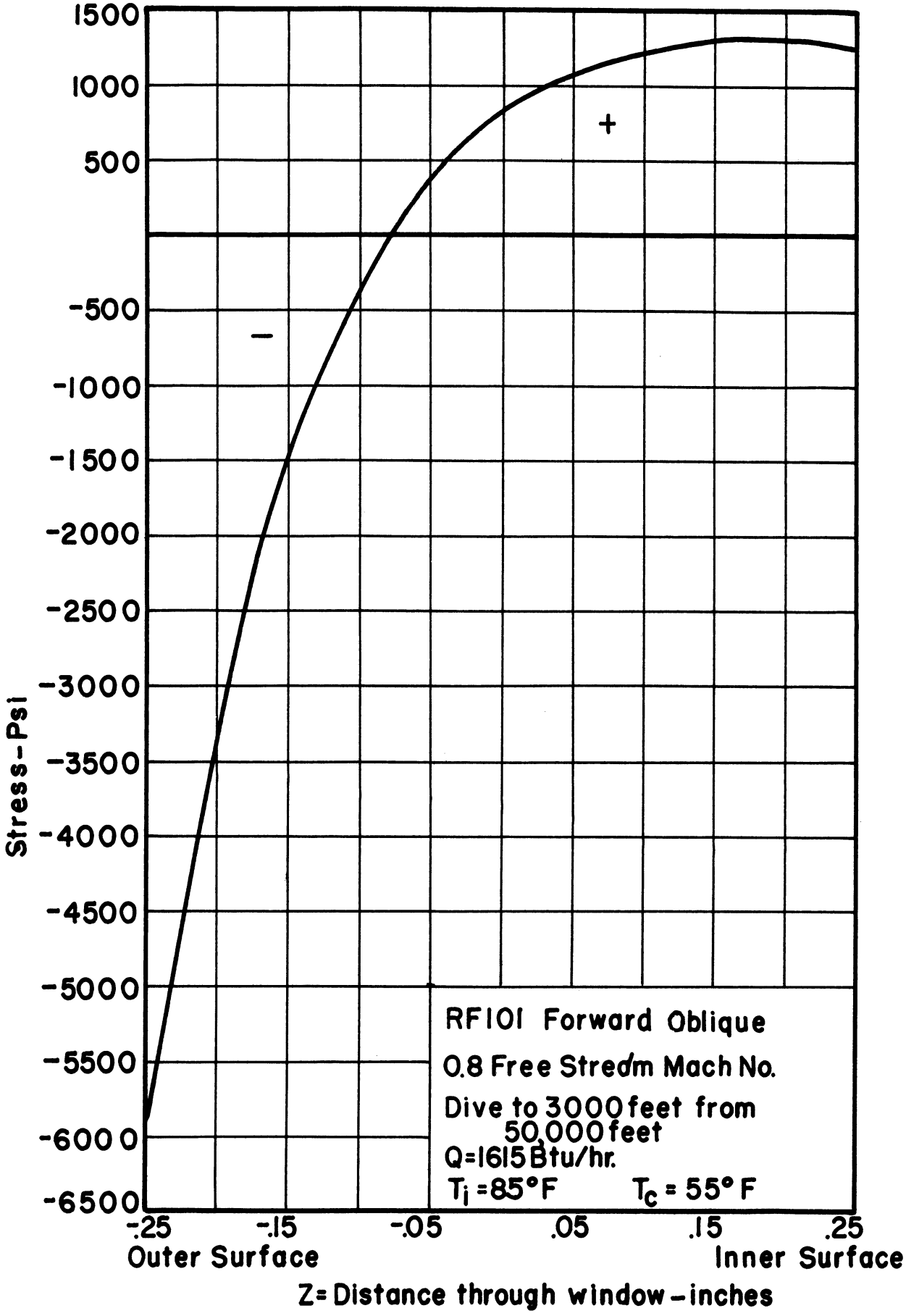

Fig. 13. Stress distribution through the RF101 forward oblique window due to thermal loading.

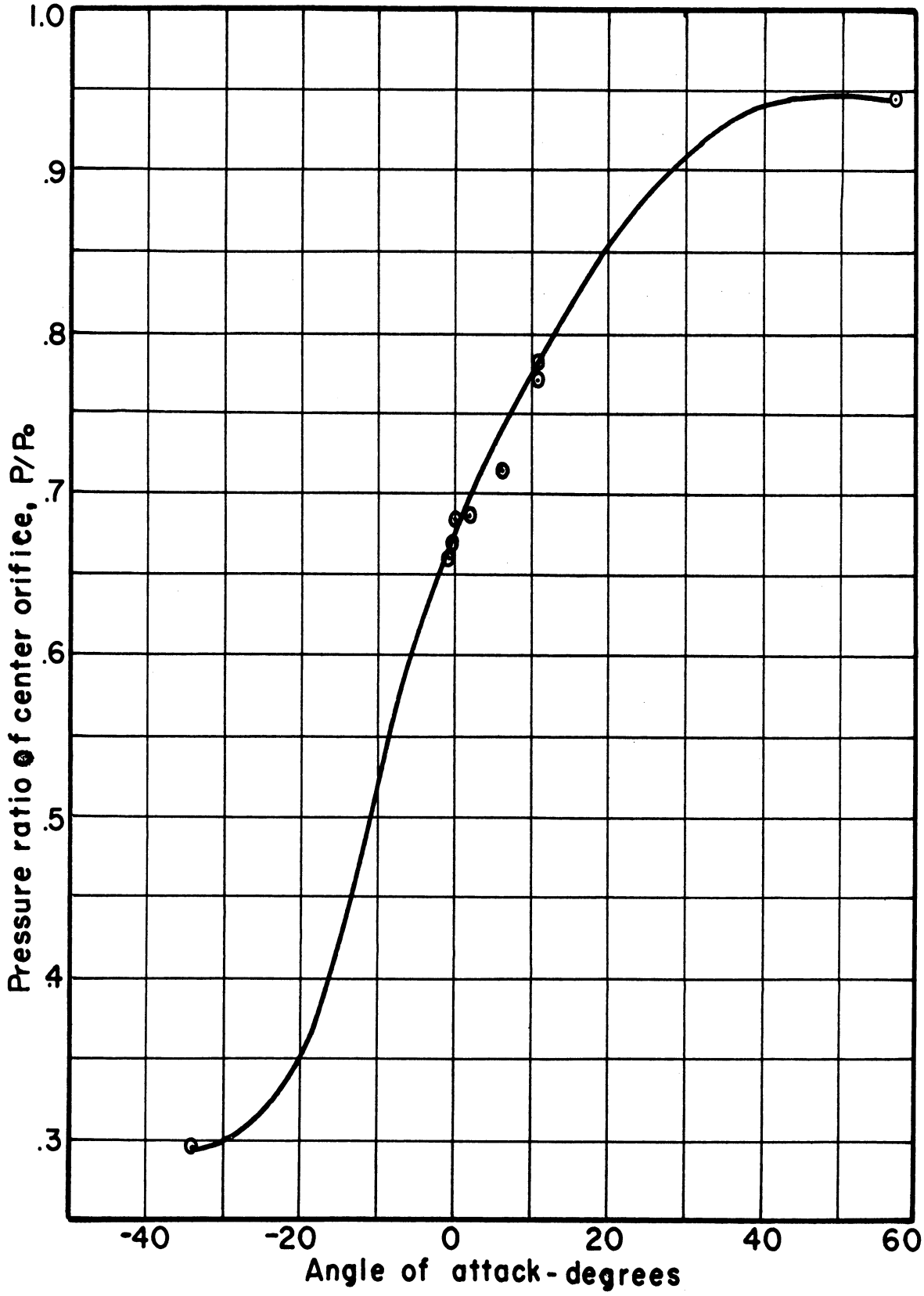

Fig. 14. Pressure distribution on RF101 forward oblique window as a function of angle of attack at Mach 1.44.

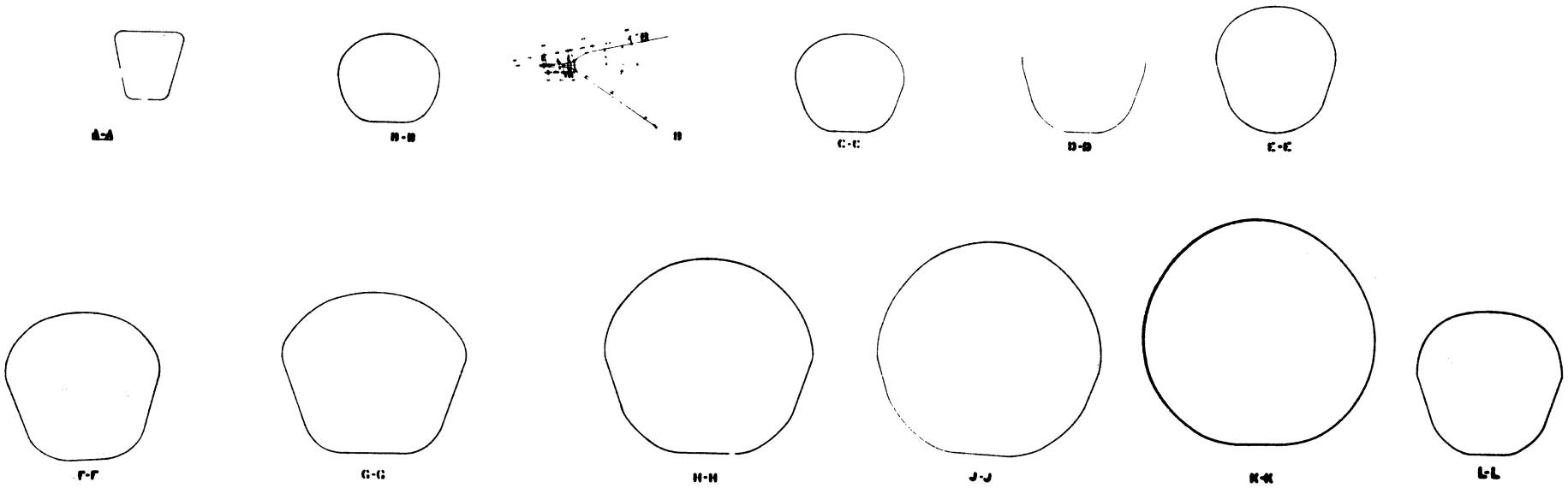

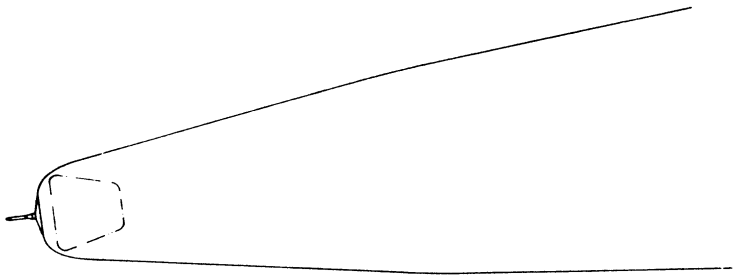

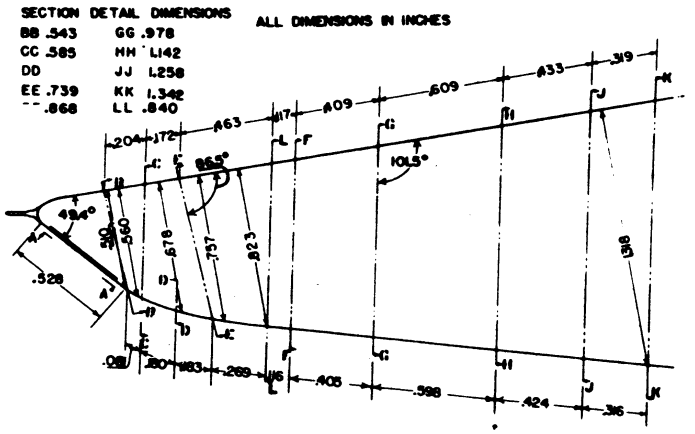

Fig. 15. Templates for scale model of RF101 nose section.